# Unsteady Wake Measurements of Airfoils and Cascades

B. Satyanarayana*
*NASA Ames Research Center, Moffett Field, Calif.*

**In the prediction methods of unsteady response of airfoils and cascades, viscous effects are neglected and the steady-state, trailing-edge Kutta condition has been assumed, although not verified as an acceptable assumption. An investigation has been undertaken to study the unsteady characteristics of airfoils and cascades at low-frequency parameters wherein the unsteady pressures, boundary layers, and wakes were measured in the presence of a sinusoidally varying gust flow. This paper presents mainly the time-mean and time-dependent wake profiles and comparisons of the wake losses obtained from the unsteady and time mean wake profiles. The chordwise unsteady pressure differentials are also presented with results showing that the differential approaches zero at the trailing edge. The experimental unsteady pressure distribution on an airfoil is also compared with the predicted distributions. The amplitudes of the unsteady pressures show good agreement except in the trailing-edge region; however, the agreement of the phase angle is poor. In the light of further studies, certain errors were observed in sectional unsteady lift and phase values presented in an earlier report. These values were recitified, and the corrected results are presented in this paper.**

## Nomenclature

$c$ = airfoil chord
$C_L$ = unsteady lift coefficient,

$$\frac{\text{lift}}{\pi\rho C U_\infty v_d} = \frac{1}{\pi}\int_0^1 (C_{p_{\text{lower}}} - C_{p_{\text{upper}}})\,\mathrm{d}\left(\frac{x}{c}\right)$$

$C_p$ = unsteady pressure coefficient, $(p-p_\infty)/\rho U_\infty v_d$
$f$ = frequency of oscillation, Hz
l.e. = leading edge
$p$ = static pressure
$S$ = cascade spacing
t.e. = trailing edge
$u$ = velocity at any general point
$U_C$ = wake centerline velocity
$U_E$ = wake edge velocity
$U_g$ = gust propagation velocity
$U_\infty$ = freestream velocity
$v_d$ = transverse gust amplitude
$W_1$ = frequency parameter based on freestream velocity and half-chord, $(\nu c/2U_\infty) = (\pi f c/U_\infty)$
$W_2$ = frequency parameter based on gust propagation velocity and half-chord, $\nu c/2U_g$
$x$ = axial distance from trailing edge
$y$ = vertical distance from chord line
$\theta$ = boundary-layer momentum thickness
$\nu$ = angular frequency, rad/sec
$\rho$ = density
$\Phi$ = phase angle between the common reference and the current reference

## Introduction

VARIOUS theoretical methods are available to predict the unsteady aerodynamic response of airfoils and cascades.[1-4] Even the most general of these methods neglect viscous effects, and the steady-state trailing-edge Kutta condition is assumed, although not accepted as a valid condition. In recent years, with the development of instrumentation for dynamic measurements, some experimental results have become available for isolated airfoils to check the validity of the predicted results.[5,6] However, no direct experimental results (such as unsteady pressure distribution or lift) have been available to check the unsteady aerodynamic characteristics of cascades.

The flow in a turbomachine is basically unsteady. The profile losses of cascades under such conditions differ from profile losses measured under steady conditions. Reference 7 shows that profile losses in an unsteady flow increase, compared with steady flow, due both to equilization of the wake downstream of the exciting cascade and to the interactions of the wake with the boundary layer. Therefore, it is important to study the wake in detail to understand the mechanism of the flow.

Experimental investigations of unsteady flow past airfoils and cascades were undertaken at the Engineering Department, University of Cambridge, England, to systematically fill this gap at low-frequency parameters. Unsteady pressures, boundary layers, and wakes were measured in the presence of a sinusoidally varying gust flow.[8] Unsteady flow visualization studies were also carried out to help understand the flow mechanism. Some of the results of the unsteady pressure measurements were presented in Ref. 9 showing that the contributions of neighboring cascade blades in an unsteady flow environment are significant. The unsteady boundary-layer measurements were reported in Ref. 10 explaining certain discrepancies observed during unsteady pressure measurements.[9]

In the present paper, the time-mean and time-dependent wake profiles of an airfoil and airfoils in cascades are presented, and the unsteady wake losses are compared with those obtained from time-mean wake profiles. The predicted unsteady pressure distribution on an airfoil is compared with experimental results. Unsteady pressure differentials near the trailing-edge region are also presented, experimentally confirming the trailing-edge condition at low-frequency parameters. The experimental unsteady lift and phase results (presented in Ref. 9) are discussed in the light of further investigations.

## Experimental Appartus

This section briefly describes the unsteady wind tunnel and its characteristics,[5,11] as well as the instrumentation and experimental techniques.[9,10] The experiments were conducted in a gust tunnel in which sinusoidal gusts were generated in a specially built 2.74-m-length (9 ft) test section whose upper and lower surfaces were flexible metal sheets (Fig. 1). These

Presented as Paper 76-7 at the AIAA 14th Aerospace Sciences Meeting, Washington, D.C., January 26-28, 1976; submitted Feb. 11, 1976; revision received Feb. 1, 1977.

Index categories: Nonsteady Aerodynamics; Jets, Wakes, and Viscid-Inviscid Flow Interactions.

*NRC Research Associate. (Formerly Scientist, National Aeronautical Laboratory, Bangalore, India.) Member AIAA.

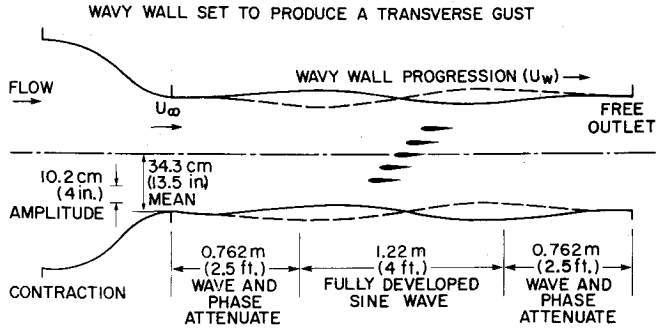


**Fig. 1 The unsteady flow wind tunnel.**

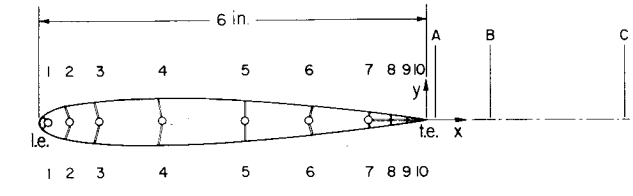


10C4 PROFILE

| STATIC PRESSURE LOCATION NO. | 1 | 2 | 3 | 4 | 5 | 6 | 7 | 8 | 9 | 10 |
|---|---|---|---|---|---|---|---|---|---|---|
| % CHORD FROM l.e. | 2.1 | 7.9 | 15.5 | 31.3 | 53.9 | 69.6 | 85.0 | 90.0 | 94.3 | 98.0 |

| WAKE MEASUREMENT LOCATION | A | B | C |
|---|---|---|---|
| DISTANCE FROM t.e. (x/c) | 0.008 | 0.150 | 0.500 |

NOTE: STATIC PRESSURE HOLE SIZE = 0.043 in.
STATIC HOLES AT 8, 9, 10 ARE CONNECTED TO THE TRANSDUCER AT LOCATION 7

**Fig. 2 Airfoil section and static hole locations.**

surfaces were deformed in the form of a sinewave by a system of cams; appropriate rotation of the cams caused the sinewave to move in the direction of the airflow. If the upper and lower surfaces were in phase, a transverse gust was produced; if the phase difference was 180°, a streamwise gust was produced. The tunnel had a width of 45.7 cm (18 in.) and a height of 68.6 cm (27 in.) in the transverse gust configuration.

The basic airfoil employed in these experiments was an unchambered NGTE 10C4 section of 15.24 cm (6 in.) chord and 45.72 cm (18 in.) span. The maximum thickness-to-chord ratio was 10%. An isolated airfoil and a cascade of five airfoils with a space/chord ratio of 0.707 and stagger angle of 45° were selected for the boundary-layer and wake measurements. The airfoils were firmly mounted between two parallel side walls in the central position of the test section. Boundary-layer roughness formed by randomly distributed glass balls of 0.356 mm (0.014 in.) diameter was applied over the central three airfoils over a width of 4.76 mm (0.187 in.) starting 7.94 mm (0.312 in.) from the leading edge. The central airfoil was instrumented with pressure transducers to measure the unsteady pressures. The space/chord radio was varied from infinity (isolated airfoil) to 0.707 with 1, 3, or 5 airfoils in position with stagger angles at 0, 22.5, or 45°.

The "Gaeltec" transducers employed were specially fabricated for the measurement of unsteady pressures over airfoils. These transducers consisted of a strain-gaged rectangular diaphragm which was located inside a long steel tube with a 3-mm (0.118 in.) diameter. A 1.09-mm-diameter (0.043 in.) hole drilled in the tube on one side of the diaphragm was aligned with the static hole on the surface of the airfoil. The transducers and the associated signal conditioning instrumentation are described in Ref. 9.

A DISA constant-temperature anemometer type 55A01, along with the hot-wire probe type 55A25, was employed for

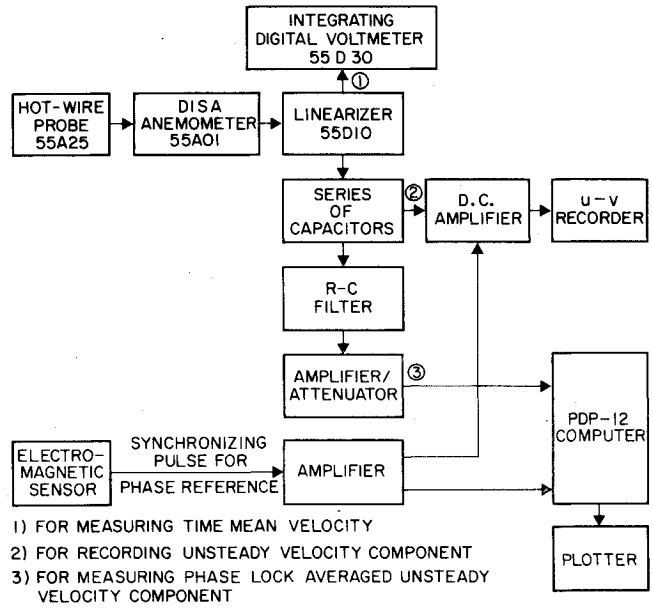


**Fig. 3 Block diagram for unsteady boundary-layer and wake measurements.**

measuing the boundary layers and wakes as described in Ref. 10. Airfoil section, transducer, and static hole locations are shown in the schematic diagram, Fig. 2.

## Data Acquisition

The pressure transducer and hot-wire data were acquired using a PDP-12 computer. Since the raw data signals from a single cycle were noisy, the data were sampled over a number of cycles, and the respective digital values were summed up to give a "phase-lock" or ensemble average. The averaged digital values were stored on the magnetic tape for further analysis. A block diagram for the wake data acquisition is shown in Fig. 3.

To initiate the data at a particular phase of the gust, a timing reference was necessary. An electromagnetic sensor was incorporated into the drive mechanism for the oscillating walls to produce a sharp electrical signal, independent of the flow conditions when the oscillating wall was at a particular position. The data sampling was always initiated at this position. This reference is defined as the common phase reference. A new reference, which is different from the common phase reference, was defined for each axial position of the wake profiles. The new phase reference corresponded to the occurrence of the maximum positive unsteady component in the freestream on the upper side of the wake. The phase angle from this new reference was zero at this instant. The new phase reference was consequently different at different chordwise positions, but it provided a consistent reference for all the profiles. The angle $\Phi$ is the phase angle difference between the common phase reference and the new phase reference. The angle $\Phi$ was determined for comparison and shown in the figures.

The wake velocity results presented in this report were obtained by a single hot-wire, aligned normal to the flow (vertical position). The time-mean hot-wire signals were measured using an integrating voltmeter. The digital voltmeter reading corresponded to the averaged value of the signal over a period of 10 sec.

Time-mean and time-dependent wake profiles were measured at the following conditions at 0.8, 15, and 50% of the chord from the tailing edge, in the wake of the isolated airfoil and cascade central blade. The freestream velocity was 15.24 m/sec (50 fps) and the ratio of the wall wave propagation velocity to the freestream velocity was 0.16. The maximum ratio of the velocity of the transverse gust to the

freestream velocity was 0.082. The Reynolds number based on the chord $c$ was 160,000, and the mean incidence of the flow was 0°. The frequency parameter of the gust $W_1$, based on the freestream velocity and the model half-chord ($\nu c/2U_\infty$), was 0.042 where $\nu$ is the angular frequency of the gust in rad/sec. The frequency parameter of the gust $W_2$, based on gust propagation velocity and model half-chord ($\nu c/2U_g$), was 0.22.

The unsteady pressures were measured over a range of geometric and aerodynamic parameters[8]; only the relevant results are discussed in this paper.

## Data Reduction and Presentation of Results

### Time-Dependent Hot-Wire Traces

Typical time-dependent hot-wire traces are presented in Fig. 4 for the airfoil and cascade. The traces are photographs of the digitized hot-wire readings that had been stored on magnetic tape for later display on the cathode ray tube on the computer. They are all presented to the same scale, 220 mV/division, for comparison of magnitude and phase. All the traces start at the common phase reference and correspond to the phase-lock averaged values.

The hot-wire traces are presented at 0.8, 15, and 50% of the chord from the trailing edge in the wakes of airfoil and cascade central blade. The phase and magnitude of the signals varied through the wake. The variations of the unsteady velocity component were quite large at some vertical positions in the wake. At each axial position in the wake, the topmost and bottommost signals represent the hot-wire traces just outside the wake (on either side). For the isolated airfoil the phase of these two signals is out of phase by 180°, whereas they are in phase for cascade at each axial position.

Similar trends were observed in the phase of unsteady pressures on the surfaces of airfoil and cascade as reported in Ref. 8. The phase of the pressure on the cascade airfoil changed by 180° at certain chordwise positions. Consequently, the phases of the pressure on the upper and lower surfaces were in phase towards the trailing-edge region of the cascade airfoil. No such abrupt change in phase of pressure occurred on the airfoil surface; consequently, they were out of phase for the isolated airfoils. Though the mean incidence of the flow was zero, there was instantaneous incidence which changed sinusoidally with time. The changes in the phase of the velocity in the wake were analogous to the changes in the phase of the pressure on the surface.

### Unsteady Wake Profiles

Instantaneous wake profiles were obtained at eight instants of time or phase angles. The hot-wire signals at various vertical positions were intercepted at the given instant of time to obtain the unsteady component to which the appropriate time-mean component was added to obtain the instantaneous profile.

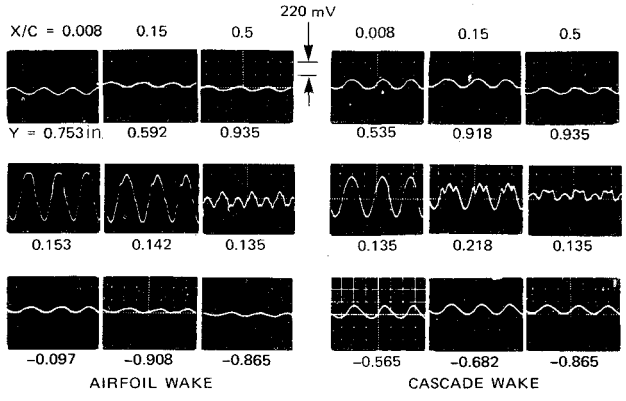


Fig. 4 Hot-wire traces in the wake at $W_1 = 0.042$.

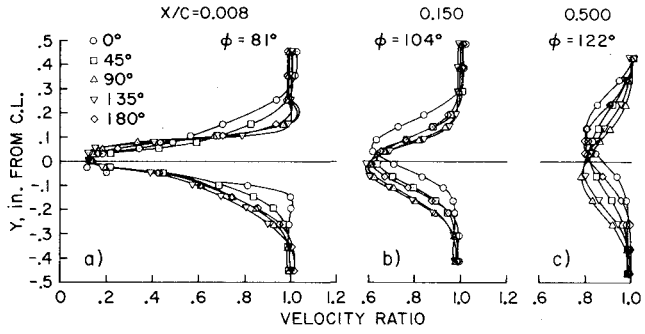


Fig. 5 Unsteady velocity profiles behind an isolated airfoil at $W_1 = 0.042$.

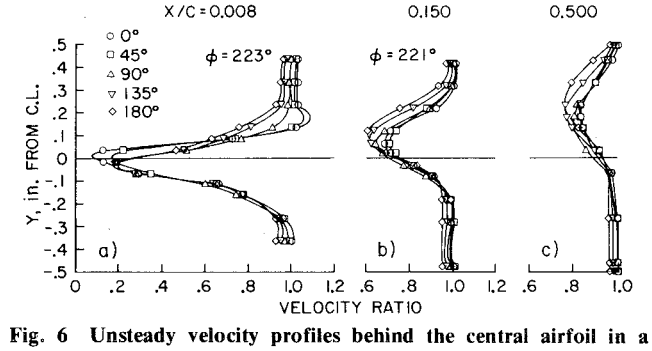


Fig. 6 Unsteady velocity profiles behind the central airfoil in a cascade at $W_1 = 0.042$.

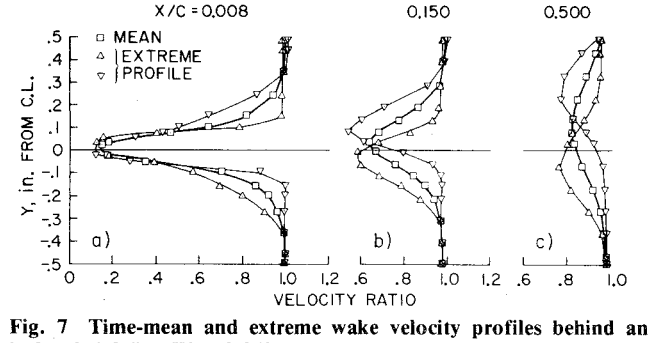


Fig. 7 Time-mean and extreme wake velocity profiles behind an isolated airfoil at $W_1 = 0.042$.

The instantaneous profiles behind an isolated airfoil are presented in Fig. 5 at 0.8, 15, and 50% of the chord from the trailing edge. The corresponding values behind the central blade of the cascade of airfoils are presented in Fig. 6. In general, the profile shifted with time. In the case of a cascade, the variation in the lower half of the profile was considerably different from the upper half. Although this could partly be attributed to the asymmetry of the cascade configuration, it was mainly attributed to the variation in the boundary-layer characteristics in the upper and lower surfaces of the cascade.

The boundary-layer characteristics changed from laminar to turbulent and back to laminar during one cycle on both surfaces of the airfoil and on the upper surfaces of the cascade, whereas the boundary layer was fully turbulent on the lower surface of the cascade.[10] These characteristics were reflected in the unsteady wake profiles.

### Time-Mean Wake Profiles

Time-mean wake profiles behind an isolated airfoil and central blade of the cascade are presented in Fig. 7 and 8, respectively. The extreme unsteady profiles are also presented in the respective figures. In the case of isolated airfoils, although there was no substantial variation in instantaneous peak velocity over a gust cycle, the peak velocity of the mean profile was smaller than the instantaneous peak velocity. This

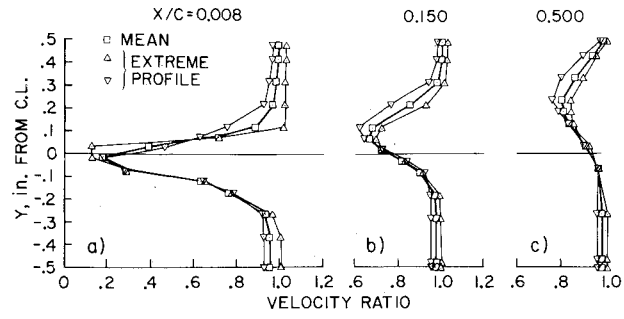


**Fig. 8 Time-mean and extreme wake velocity profiles behind the central airfoil in cascade at $W_1 = 0.042$.**

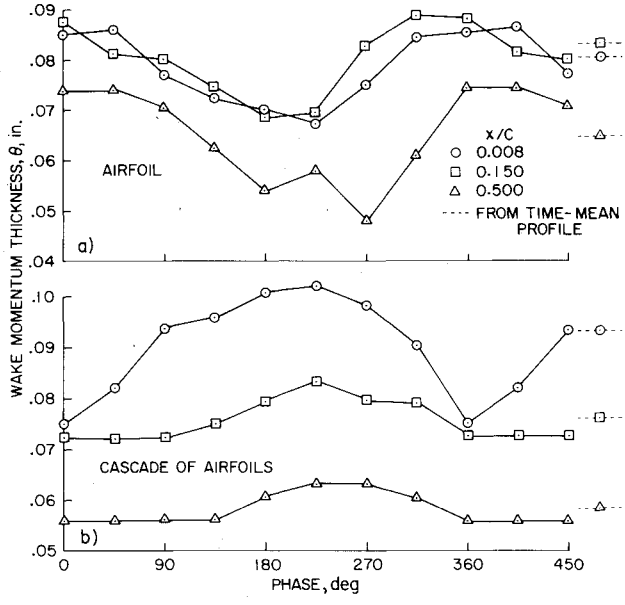


**Fig. 9 Variation of the wake momentum thickness with phase of the gust.**

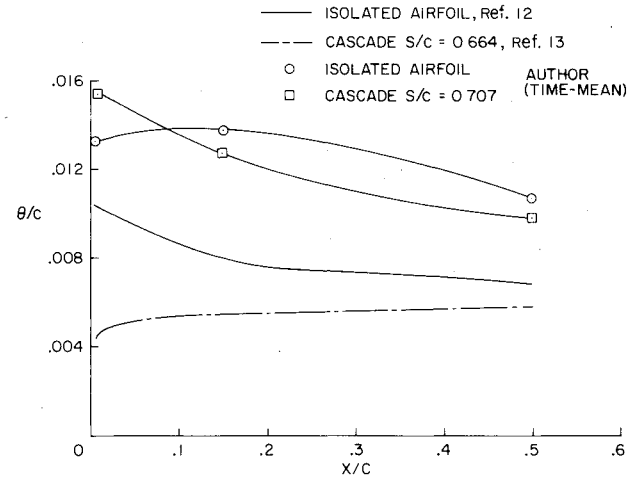


**Fig. 10 Variation of wake momentum thickness with downstream distance.**

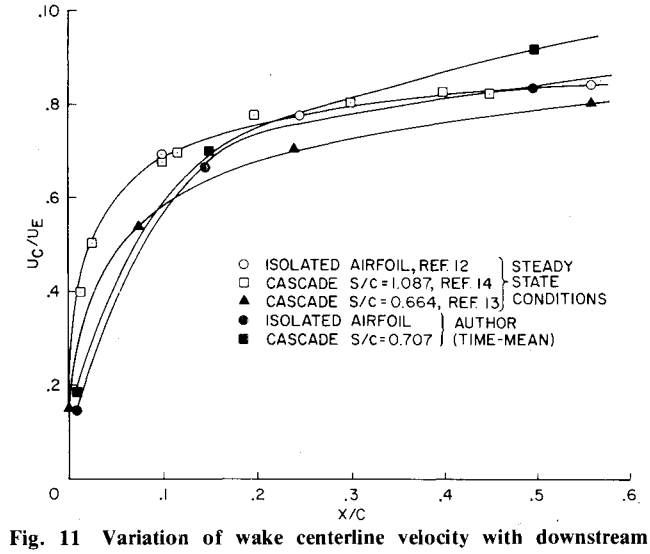


**Fig. 11 Variation of wake centerline velocity with downstream distance.**

was due to the large vertical shift of the profiles with time. In the case of the cascade, the vertical shift was smaller; consequently, the mean peak value corresponded to the average value.

## Discussion

### Unsteady Wake Losses

The wake momentum thickness $\theta$ was evaluated using the formula

$$\theta = \int \frac{u}{U_E}\left(1 - \frac{u}{U_E}\right) dy$$

where $u$ is the axial velocity component inside the wake and $U_E$ is the wake edge velocity. The variations of the momentum thickness with phase of the gust are presented in Figs. 9a and 9b for the airfoil and the cascade, respectively. The results are presented for three axial positions. The momentum thickness calculated from the time-mean profiles is also shown on the figures for comparison. The results indicate that the unsteady value of the momentum thickness varied as much as +25% to −15% from the time-mean value. The steady-state value could also differ from the time-mean value. This indicated the importance of the measurements of unsteady profiles for the realistic evaluation of the unsteady drag coefficient.

Variations of $\theta$ with downstream are shown in Fig. 10. The steady-state values of Preston, Sweeting, and Cox[12] for an isolated airfoil and those of Raj and Lakshminarayana[13] for a cascade are presented in the same figure. Apart from the differences noted due to the geometry,[13] the unsteady nature of the flow also contributed to the deviation in $\theta$ and drag coefficient.

The variation of the wake centerline velocity (time-mean value) with downstream distance is shown in Fig. 11 and is compared with the steady-state results.[12-14] At the center of the wake close to the trailing edge, the time-mean velocity of the unsteady wake is smaller than the velocity of the steady wake. But at a distance of 50% of the chord length from the trailing edge, the mean velocity of the unsteady wake is higher compared to the steady wake velocity. From the experimental results it was observed that the unsteady wake centerline velocity deviated from the time-mean velocity by as much as 10% of the wake edge velocity. It was also noted that the wake edge velocity decreased with downstream distance (by about 3% at half-chord length) in the case of the cascade, whereas there was a slight increase (0.6%) for the isolated airfoil.

### Trailing-Edge Condition

To obtain a unique solution for theoretical predictions of pressure distribution, the Kutta condition of zero pressure differential is often imposed at the trailing edge. The definition and applicability of trailing-edge conditions are discussed in Ref. 15 for various geometric and aerodynamic conditions. In this section, the Kutta condition is examined in

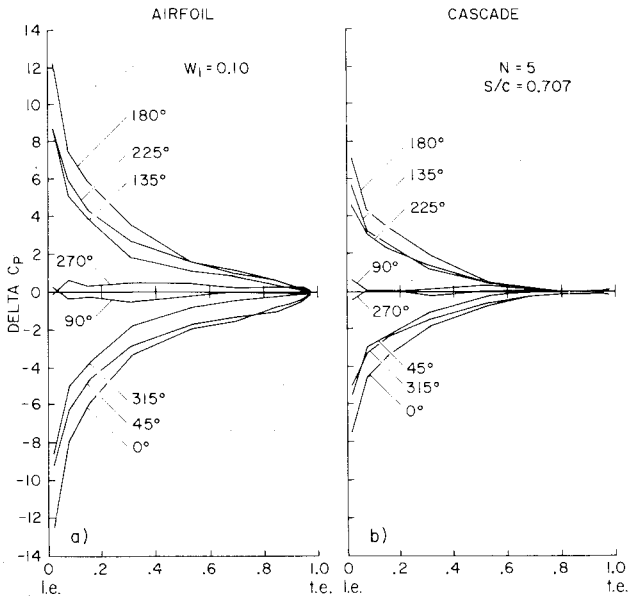


Fig. 12 Typical chordwise unsteady pressure differential at various instants of time in a cycle. $Re = 80{,}000$ without boundary-layer trip.

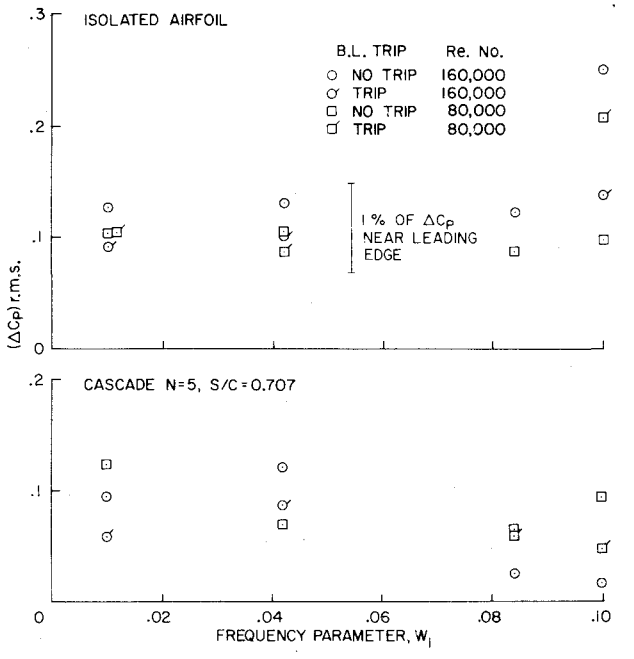


Fig. 13 The variation of rms pressure differential at 98% chord pressure with frequency parameter.

the light of the experimental results at low-frequency parameters. Unsteady pressures were measured at 85, 90, 95, and 98% of the chord in the trailing-edge regions on the upper and lower surfaces of an isolated airfoil and on the central airfoil of the cascade. The pressure in this region was measured using the transducer located at 85% of the chord, communicating one static hole at a time and blocking the other static holes with cellotape.

Typical chordwise pressure differentials at various instants of time in a cycle are presented in Figs. 12a and 12b for the isolated airfoil and cascade, respectively. It can clearly be observed that the instantaneous pressure differential was very low and approached zero at the trailing edge for all the conditions tested. While the instantaneous pressure difference was low, the absolute level of pressure (unsteady component) at the trailing edge fluctuated appreciably, particularly for the cascade.[9]

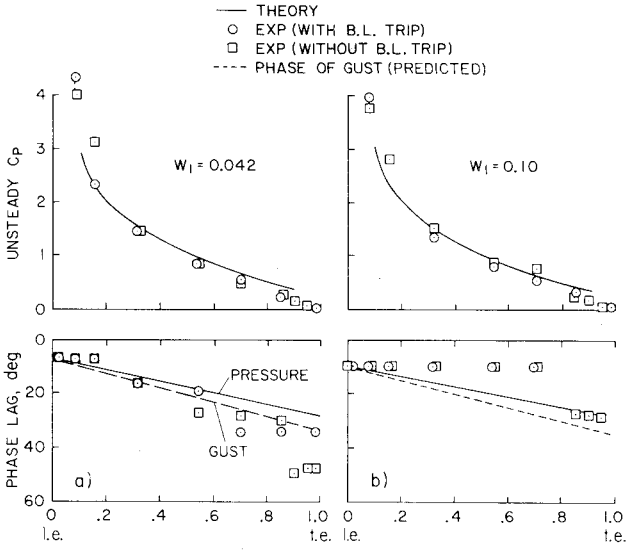


Fig. 14 Comparison of experimental unsteady pressure and phase distribution with predicted results for an isolated airfoil.

The rms values of the pressure differential over a cycle at 98% of the chord are presented in Fig. 13 for various frequency parameters. Note that the level of pressures at the trailing edge was very small (on the order of 4-5% of the peak unsteady pressures). The resolution of the differential pressure at the trailing edge was therefore not good—being the difference of these two small quantities. Though it was difficult to predict any trends in this range of frequency parameters, it could reasonably be concluded that the assumption of instantaneous zero pressure differential at the trailing edge was valid within the accuracy of these measurements.

### Comparison of Unsteady Pressure Distribution

Holmes[5] developed a computer program for determining the pressure distribution on an isolated airfoil in the presence of nonconvected gusts. The experimental chordwise unsteady pressure and phase distribution were compared with predicted results obtained using this program. Results at two frequency parameters are presented in Figs. 14a and 14b. The variations of the phase of the gust in the absence of the model are also presented in the figures, starting at the same point at the leading edge. The experimental pressure distribution agreed reasonably well with the predicted results except in the trailing-edge region. The discrepancy in the trailing-edge region could be attributed to the viscous effects, since the predicted results were based on the potential theory. At a reduced frequency of $W_1 = 0.042$, the phase of the pressure was in tune with the gust, whereas, at $W_1 = 0.1$, the phase was tuned to a common phase except at the trailing edge. Although experimental errors were partly responsible for the deviations, the discrepancies in phase between theory and experiment could possibly be due to the representation of the wake flow in the prediction methods, since wake was assumed to be rectilinear, and it propagated with the freestream velocity.

### Unsteady Lift Distribution

The unsteady lift and phase in the presence of nonconvected sinusoidal gusts are predicted and compared with typical experimental results in Fig. 8 and 9 of Ref. 9. The unsteady lift distribution was obtained by integrating the measured chordwise unsteady pressures. There were two major discrepancies in the results presented in Ref. 9. One of these discrepancies was the predicted lift coefficient; the intrablade frequency $\tau$ was defined as $2(s/c)\,W_1 \sin\xi$ instead of the correct value $-2(s/c)\,W_1 \sin\xi$ where $\xi$ is the stagger angle of the cascade. However, the computer calculation of the lift

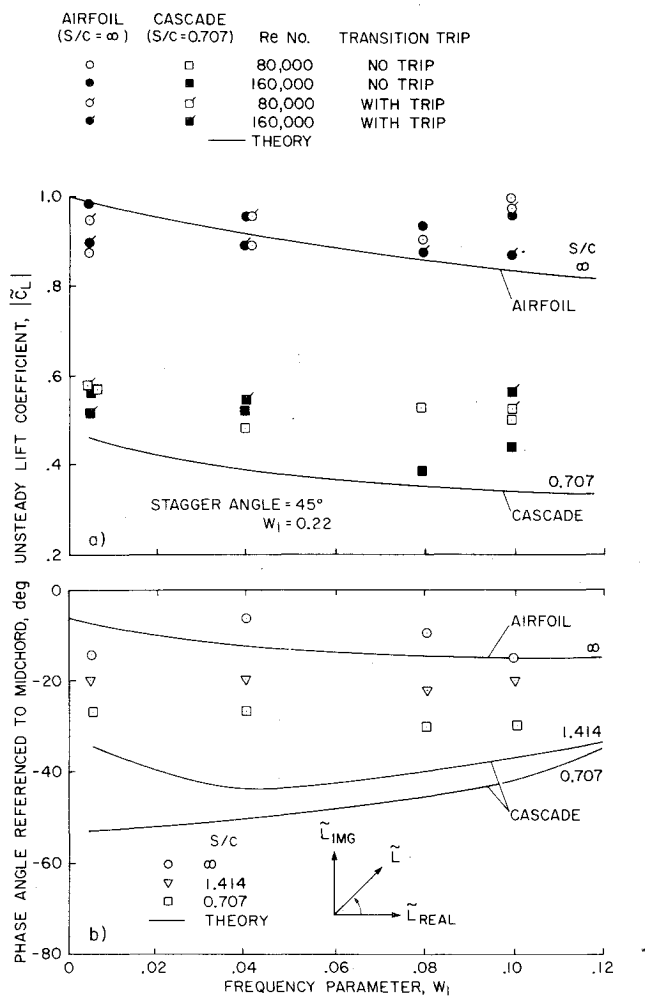


**Fig. 15 Variation of unsteady lift amplitude and phase with frequency parameter.**

coefficient was carried out using $-2(s/c)\ W_1 \csc\xi$. As such, the predicted lift coefficient was in error. The second discrepancy was the experimental phase of the unsteady lift; a phase lag in the signal conditioning system was subsequently observed which was not taken into account in the results presented in Ref. 7. These errors have have been rectified and the correct results of the magnitude and phase of the unsteady lift are presented in Figs. 15a and 15b, respectively. With these corrections, the agreement with the phase was improved, though the deviations in the lift magnitude were larger. The deviation in the results could be attributed to the viscous effects and the deficiency in the representations of the theoretical model. The errors in the measurements and the blockage of the model also contributed to the deviations.

## Conclusions

1) Time-mean profiles were different from unsteady wake profiles. The time-mean centerline velocity was considerably smaller where there was a vertical shift in the unsteady profiles. This will affect the profile drag as observed from momentum thickness of the wake profiles.

2) The assumption of zero pressure differential at the trailing edge of the airfoil or airfoils in a cascade was experimentally verified at low-frequency parameters. Similar measurement and analyses techniques are useful to extend the work to higher frequency parameters.

3) The predicted unsteady pressure distributions on an airfoil compared reasonably well with the experimental results (except in the trailing-edge region), but the results of phase distribution differed.

4) There was a deviation in the magnitude of the predicted and experimental lift results for a cascade, although good agreement was present in trends. These deviations were attributed to the viscous effects and the deficiency in the representation of the theoretical model.

## Acknowledgments

The experimental work, supported by the Procurement Executive, U.K. Ministry of Defense, was performed as part of the author's Ph.D. program at Cambridge University, England. The author wishes to acknowledge the helpful advice and encouragement of J. P. Gostelow, J. H. Horlock, and R. E. Henderson during the course of this work. The author is grateful to C. F. Coe, NASA Ames, for his helpful suggestions in preparing this paper.

## References

[1]Sears, W. R., "Some Aspects of Non-Stationary Airfoil Theory," *Journal of the Aerospace Sciences*, Vol. 8, Jan. 1941, pp. 104-108.

[2]Horlock, J. H., "Fluctuating Lift Forces in Aerofoils Moving Through Transverse and Chordwise Gusts," *Transactions of the ASME: Journal of Basic Engineering*, Vol. 90D, 1968, pp. 494-500.

[3]Whitehead, D. S., "Force and Moment Coefficients for Vibrating Aerofoils in Cascade," Aeronautical Research Council, London, Reports and Memoranda 3254, 1960.

[4]Henderson, R. E. and Daneshyar, H., "Theoretical Analysis of Fluctuating Lift on the Rotor of an Axial Turbomachine," Reports and Memoranda 3684, 1972, Aeronautical Research Council, London.

[5]Holmes, D. W., "Lift Fluctuations on Aerofoils in Transverse and Streamwise Gusts," Ph.D. Dissertation, Engineering Dept., University of Cambridge, England, Oct. 1972.

[6]Carta, F. O. and Commerford, G. L., "Unsteady Aerodynamic Response of a Two-Dimensional Airfoil at High Reduced Frequency," *AIAA Journal*, Vol. 12, Jan. 1974, pp. 43-48.

[7]Samoilovich, G. S. and Yablokov, L. D., "Profile Losses with Unsteady Flow Through Turbomachine Cascades," *Teploenergetika*, Vol. 18(A), 1971, pp. 73-75.

[8]Satyanarayana, B., "Unsteady Flow Past Aerofoils and Cascades," Ph.D. Dissertation, Engineering Dept., University of Cambridge, England, March 1975.

[9]Satyanarayana, B., Henderson, R. E., and Gostelow, J. P., "A Comparison Between Experimental and Theoretical Fluctuating Lift on Cascades at Low Frequency Parameters," Paper 74-GT-78, *presented at the ASME Gas Turbine Conference*, March 30-April 4, 1974, Zurich, Switzerland.

[10]Satyanarayana, B., "Some Aspects of Unsteady Flow Past Airfoils and Cascades," Paper 25, *presented at the 46th Meeting of AGARD Propulsion and Energetics Panel*, September 22-26, 1975, Monterey, Calif.

[11]Horlock, J. H., "An Unsteady Flow Wind Tunnel," *Aeronautical Quarterly*, Vol. XXV, May 1974, pp. 81-90.

[12]Preston, J. H., Sweeting, N. E., and Cox, D. K., "The Experimental Determination of the Boundary Layer and Wake Characteristics of a Piercy 12/40 Aerofoil, with Particular Reference to the Trailing Edge Region," Aeronautical Research Council, London, Reports and Memoranda No. 2013, 1945.

[13]Raj, R. and Lakshminarayana, B., "Characteristics of the Wake Behind a Cascade of Airfoils," *Journal of Fluid Mechanics*, Vol. 61, Part 4, 1973, pp. 707-730.

[14]Lieblein, S. and Roudebush, W. H., "Low-Speed Wake Characteristics of Two-Dimensional Cascade and Isolated Airfoil Sections, NACA TN 3771, 1956.

[15]Gostelow, J. P., "Trailing Edge Flows Over Turbomachine Blades and the Kutta-Joukowsky Conditions," Paper 75-GT-94, *presented at the 20th ASME International Gasturbine Conference*, March 2-6, 1975, Texas.